Communications

Nonisothermal Growth and Dissolution of Inclusions in Liquid Steels

T. HONG and T. DEBROY

The thermodynamic stability and diffusion-controlled growth and dissolution of inclusions have received considerable attention in the literature.[1,2] However, synthesis of the accumulated knowledge of the thermodynamics and the kinetics of inclusion growth and dissolution has been mostly overlooked. There are many instances where such synthesis has enormously facilitated practical use of fundamental knowledge. For example, the time-temperature-transformation (TTT) diagrams have become important tools in metallurgy for understanding phase transformation behavior in alloys.

Synthesis of our current knowledge of the thermodynamics and kinetics of inclusion growth and dissolution can provideimportant information about the behavior of inclusions in steels. In recent articles,[3,4] we showed that the effects of time and temperature on the growth and dissolution behavior of inclusions in liquid steels can be represented by a set of TTT diagrams. Apart from the stability of various inclusions in a given composition of steel, the diagrams provide important kinetic information about diffusion-controlled growth and dissolution of inclusions. Although the TTT diagrams are restricted to isothermal behavior, here, we show how they can be readily extended to inclusion growth and dissolution in nonisothermal conditions. The Scheil additive rule,[4,5] a well-known approach, can be used to calculate the continuous cooaling transformation (CCT) diagrams for the growth and continuous heating transformation (CHT) diagrams for the dissolution from the corresponding TTT diagrams. The approach and calculated results presented here reveal the effects of time and temperature on the inclusion growth kinetics during continuous cooling and inclusion dissolution kinetics during continuous heating.

References 3 and 4 describes the method of calculating the TTT diagrams for the growth and dissolution of oxide, nitride, and sulfide inclusions in steels and it will not be repeated here. Instead, only the salient features of the calculations needed to understand the construction of the proposed CCT and CHT diagrams are presented here. The growth and dissolution rates of spherically shaped inclusions are assumed to be controlled by the diffusion of nonmetallic constituent elements in liquid steels. This assumption is based on the finding that in the temperature range 1823 to 1873 K, the silicon- and aluminum-assisted deoxidation rates of iron alloys were found to be controlled by mass transfer of oxygen within the melt.[6] It is also assumed that the oxygen and aluminum concentrations in the weld metal do not change significantly during the growth of inclusions. This assumption would be valid where there is insufficient supersaturation for homogeneous nucleation and nucleation occurs at a finite number of heterogeneous nucleation sites. During welding, the atomic oxygen gas from the plasma dissolves continuously in the weld metal at a very rapid rate. As a result, the oxygen that is depleted due to formation of the inclusions is replenished by the dissolution of oxygen in the weld metal from the plasma. Because the atomic oxygen is much more reactive than the diatomic oxygen, and the weld pool is well mixed, the concentration of dissolved oxygen in the weld pool is determined by the thermodynamic equilibrium between the atomic oxygen gas in the plasma and the dissolved oxygen in the liquid weld metal. The concentrations of the elements at the interface between the inclusions and the liquid steel are needed to calculate the diffusion rates at various temperatures. The method of calculating interfacial concentrations at a constant temperature is indicated in References 3 and 4. After the interfacial concentrations are known, a dimensionless concentration of nonmetallic elements, c^*, may be defined as[7]

$$c^* = (c_Q^b - c_Q^i)/(c_Q^P - c_Q^i) \qquad [1]$$

where c_Q is the concentration of nonmetallic element Q; and the subscripts p, b, and i refer to the inclusion particle, bulk liquid metal, and inclusion/steel interface, respectively. Because the concentration of Q in the inclusion particle, c_Q^P is always higher than that at the interface, c_Q^i, the sign of c^* depends on the relative values of c_Q^b and c_Q^i. When the temperature is lower than the equilibrium temperature for the coexistence of the inclusion and the liquid steel, c_Q^b is higher than c_Q^i and, as a result, c^* is positive. In this situation, the element Q is transported from the bulk liquid toward the interface resulting in inclusion growth. Equation [2] is applied to calculate the growth behavior in this case.[7]

$$r_{i+l} - r_i = \frac{\sqrt{2D_Q c^*}}{2\sqrt{t}}\Delta t \qquad [2]$$

When the temperature is higher than the equilibrium temperature for the coexistence of inclusion and liquid steel, c^* is negative and the element Q diffuses from the interface into the bulk liquid. The dissolution rate of the inclusion is given by.[8]

$$r_{i+1} - r_i = c^*\left[\frac{D_Q}{r_i} + \sqrt{\frac{D_Q}{\pi t}}\right]\Delta t \qquad [3]$$

In Eqs. [2] and [3], r_i and r_{i+1} are the inclusion radii before and after the ith time-step, respectively; Δt is the time-step; and D_Q is the temperature-dependent diffusion coefficient of Q in liquid steel calculated by

$$D_Q = D_Q^0 \cdot e^{-(E/RT)} \qquad [4]$$

where D_Q^0 is a temperature-independent pre-exponential term and E is the activation energy for diffusion.

The TTT diagrams are largely restricted to isothermal situations, but they can be extended to predict the nonisothermal behavior from the isothermal transformation curves.

T. HONG, formerly Graduate Student with the Department of Materials Science and Engineering, The Pennsylvania State University, is Senior Project Engineer with the Technical Center, Caterpillar Inc., Peoria, IL 61656. T. DEBROY, Professor, is with the Department of Materials Science and Engineering, The Pennsylvania State University, University Park, PA 16802. Contact e-mail: debroy@psu.edu

Manuscript submitted January 22, 2001.

The goal is to construct CCT or CHT curves from the isothermal TTT curves using the Scheil additive rule. In this procedure, the total time to reach a specified stage of transformation (final size in the case of inclusion growth and dissolution) is obtained by adding the fractions of time to reach this stage isothermally until the sum reaches unity. The additive rule[5] can be expressed by Eq. [5]:

$$\int_0^t \frac{dt}{t_i(T)} = 1 \qquad [5]$$

where $t_i(T)$ is the time needed for isothermal growth or dissolution to a specified extent at a temperature T, t is the time to that extent for the nonisothermal growth or dissolution, and dt is the time interval during heating or cooling. The data used in the calculations are presented in Tables I and II.

The TTT curve in Figure 1 shows the time necessary for an Al_2O_3 inclusion to reach the target final radius (r_t = 3 μm) at various temperatures during isothermal growth. It is also observed that the TTT diagrams show the characteristic "C" shape. The growth rate of inclusions depends on the diffusion coefficient, D_O, and dimensionless supersaturation, c^*, as can be observed from Eq. [2]. When the temperature decreases from the equilibrium temperature for the inclusion/alloy system, the supersaturation increases and the diffusion coefficient decreases. As a result, there is an optimal temperature where the growth rate is fastest. The strong effect of temperature on the growth is also observed from the figure. When the temperature is above the equilibrium temperature for the inclusion/alloy system, the inclusions will dissolve. The isothermal and nonisothermal dissolution kinetics will be discussed subsequently in this article.

The CCT curve in Figure 1 shows the time necessary to reach the same target radii for cooling from an arbitrarily assumed initial temperature of 2200 K. The computed CCT diagram shows some characteristics that are similar to the TTT diagram. For example, both plots show strong effects of time and temperature. At relatively high temperatures, the CCT curve shifts to the right. Therefore, both the TTT and the CCT diagrams for the growth of Al_2O_3 are somewhat similar in shape to those of the CCT and TTT diagrams for the decomposition of austenite in steels.[9] The cooling curves considered in Figure 1 correspond to an initial temperature of 2200 K and constant cooling rates of 250 and 125 K/s. It is observed that at 250 K/s, the cooling curve does not intersect with the CCT diagram. As a result, it is not possible for an inclusion to growth to 3-μm radius while undergoing a constant cooling rate of 250 K/s starting from an initial temperature of 2200 K. In contrast, if an inclusion were to cool at 125 K/s starting from the same temperature, the inclusion could grow to 3-μm radius in slightly over 3 seconds, as indicated by the intersection of the cooling curve with the CCT diagram.

Figure 2 shows the TTT and CCT curves for Al_2O_3 inclusions of various final target radii of 1, 3, and 5 μm. The effect of cooling rate on the growth of a particular size of Al_2O_3 inclusion can be easily calculated from this figure. For example, while cooling at a rate of 200 K/s from an initial 2200 K, the radius of an Al_2O_3 inclusion can reach 1 μm but not 3 μm. However, when the cooling rate becomes

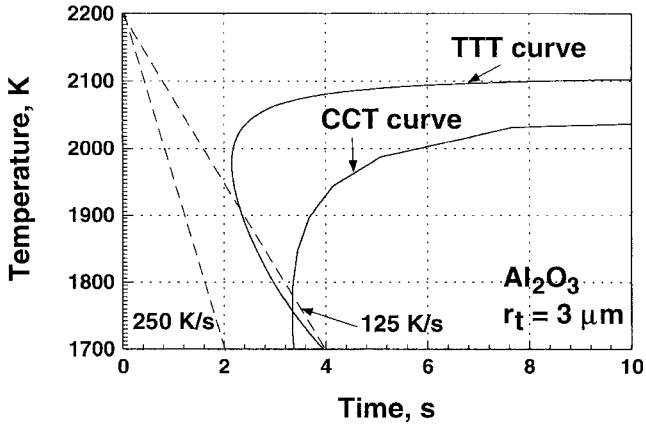

Fig. 1—CCT and TTT diagrams for the growth of Al_2O_3 inclusions to a target radius of 1 μm in a liquid alloy of the following composition: 0.09 pct C-053 pct Si-1.9 pct Mn-0.09 pct Ni-0.01 pct Cr-0.005 pct Ti-0.010 pct Al-0.008 pct N-0.032 pct O-0.020 pct S

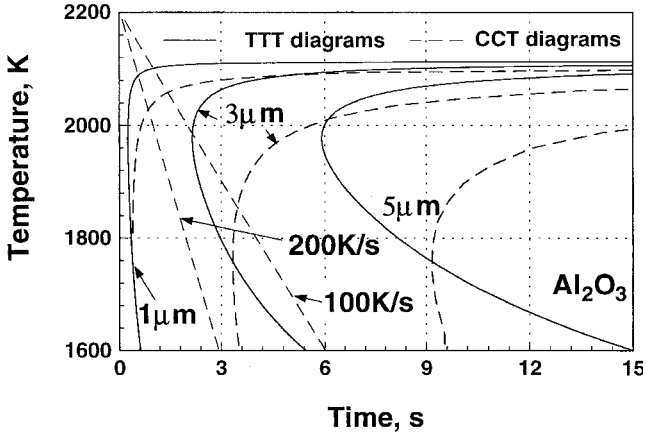

Fig. 2—CCT and TTT diagrams for the growth of Al_2O_3 inclusions to various target radii in an alloy of composition indicated in Table II.

Table I. Standard Free Energy for Various Reactions[10,11] $\Delta G^\circ = a + bT$, kJ/mole

Precipitation Reaction	A	B
$2\underline{Al} + 3\underline{O} = Al_2O_3$	−1209	0.391
$3\underline{Ti} + 5\underline{O} = Ti_3O_5$	−1756	0.571
$\underline{Ti} + 2\underline{O} = TiO_2$	−675.6	0.234

Table II. Alloy Composition and Diffusion Coefficient of Oxygen Used in the Calculations[12,13]

Element	C	Si	Mn	Ni	Cr	Ti	Al	N	O	S
Concentrations (wt Pct)	0.09	0.53	1.9	0.09	0.01	0.005	0.010	0.008	0.032	0.020
$D_{1873K} = 1 \times 10^{-8}$ m^2/s							E = 72.5 kJ/mol			

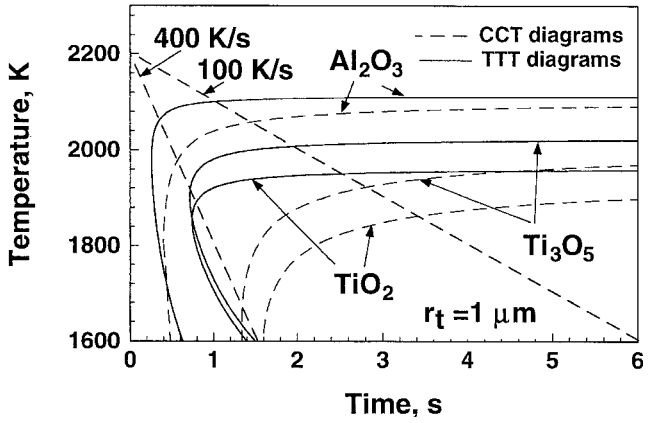

Fig. 3—CCT and TTT diagrams for the growth of several oxide inclusions to a target radius of 1 μm in an alloy of composition indicated in Table II.

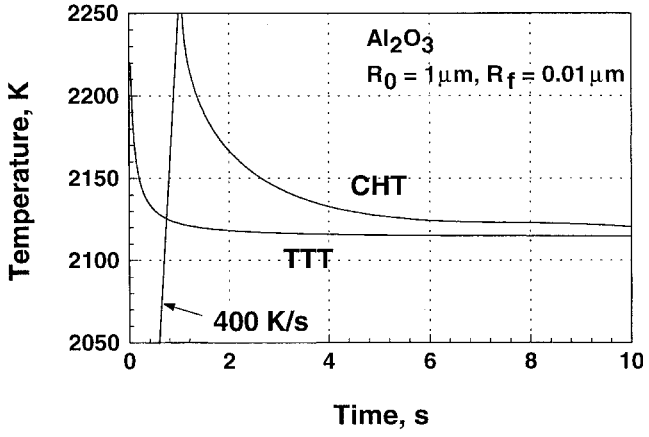

Fig. 4—CHT and TTT diagrams for the dissolution of Al_2O_3 inclusions from the initial radius 1 μm to a radius of 0.01 μm in an alloy of composition indicated in Table II.

100 K/s, the inclusion can grow to 3 μm in about 3 seconds. The TTT and CCT curves for several types of oxide inclusions growing to the same final target radius 1 μm are shown in Figure 3. Using this diagram, it is possible to calculate if a certain type of inclusion will growth to a target size at a fixed cooling rate. For example, cooling from 2200 K at a fixed cooling rate of 400 K/s, the Al_2O_3 and Ti_3O_5 inclusions of 1-μm radius can form in the liquid steel but TiO_2 cannot grow to this size at this cooling rate. However, at a cooling rate of 100 K/s, all three types of inclusions can grow to 1-μm radius in less than 4 seconds.

The TTT curve in Figure 4 shows the time necessary for an Al_2O_3 inclusion to dissolve from the original size of 1-μm radius to 1 pct of original radius at various temperatures during isothermal dissolution. The CHT curve shows the time necessary to dissolve the inclusion during heating from 1800 K. It is observed that at a constant heating rate of 400 K/s, the heating curve does not intersect with the CHT diagram, indicating that an inclusion of 1-μm radius will not be completely dissolved when heated to 2250 K.

The nonisothermal behavior of growth and dissolution of inclusion can be predicted from their isothermal growth behavior by constructing CCT diagrams for growth and CHT diagrams for dissolution. This approach offers tools to better understand the effects of temperature and time on the growth and dissolution of inclusions in liquid steels under nonisothermal conditions.

The present study was supported by Division of Materials Sciences, Office of Basic Energy Sciences, the United States Department of Energy, under Grant No. DE-FG02-84ER45158.

REFERENCES

1. S.S. Babu, S.A. David, J.M. Vitek, K. Mundra, and T. DebRoy: *Mater. Sci. Technol.*, 1995, vol. 11, pp. 186-99.
2. O. Kluken and O. Grong: *Metall. Trans. A*, 1989, vol. 20A, pp. 1335-49.
3. T. Hong and T. DebRoy: *Scripta Mater.*, 2001, vol. 44, pp. 847-52.
4. T. Hong and T. DebRoy: *Ironmaking and Steelmaking,* 2001, vol. 28 (6), pp. 450-54.
5. E. Scheil: *Arch. Eisenhuttenwes.*, 1935, vol. 12, pp. 565-67.
6. A.L. Kundu, K.M. Gupt, and P.K. Rao: *Ironmaking and Steelmaking*, 1986, vol. 13, pp. 9-15.
7. J.W. Christian: *The Theory of Transformations in Metals and Alloys—Part I: Equilibrium and General Kinetic Theory*, 2nd ed., Pergamon Press, Oxford, United Kingdom, 1981, pp. 544-45.
8. M.J. Whelan: *Met. Sci. J.*, 1969, vol. 3, pp. 95-97.
9. Z. Yang and T. DebRoy: *Metall. Trans. B*, 1999, vol. 30B, pp. 483-93.
10. E.T. Turkdogan: *Physical Chemistry of High Temperature Technology*, Academic Press, New York, NY, 1980, pp. 31-57.
11. G.K. Sigworth and J.F. Elliott: *Met. Sci. J.*, 1974, vol. 8, pp. 298-310.
12. G.H. Geiger and D.R. Poirier: *Transport Phenomena in Metallurgy*, Addison-Wesley Publishing Company, Reading, MA, 1987, p. 498.
13. F.D. Richardson: *Physical Chemistry of Melts in Metallurgy*, Academic Press, London, 1974, p. 413.